

Equation of state and Taylor expansions at nonzero isospin chemical potential

Bastian B. Brandt,^{a,*} Francesca Cuteri^b and Gergely Endródi^a

^a*Institute for Theoretical Physics, University of Bielefeld, D-33615 Bielefeld, Germany*

^b*Institute for Theoretical Physics, Goethe University, D-60438 Frankfurt am Main, Germany*

E-mail: brandt@physik.uni-bielefeld.de, endrodi@physik.uni-bielefeld.de, cuteri@itp.uni-frankfurt.de

We compute the equation of state of isospin asymmetric QCD at zero and non-zero temperatures using direct simulations of lattice QCD with three dynamical flavors at physical quark masses. In addition to the pressure and the trace anomaly and their behavior towards the continuum limit, we will particularly discuss the extraction of the speed of sound. Furthermore, we discuss first steps towards the extension of the EoS to small non-zero baryon chemical potentials via Taylor expansion.

*The 39th International Symposium on Lattice Field Theory,
8th-13th August, 2022,
Rheinische Friedrich-Wilhelms-Universität Bonn, Bonn, Germany*

*Speaker

1. Introduction

The equation of state constitutes the most relevant input for the phenomenological description of physical systems in cosmology and astrophysics and is essential for the hydrodynamical modeling of heavy-ion collisions. Most of these systems are dominated by non-vanishing baryon density, but charge and strangeness densities can also contribute significantly to the thermodynamics of the system. For some systems it is indeed the charge density which plays the major role, such as in the case of an early Universe featuring sizeable lepton flavour asymmetries [1–3]. In all of these cases, however, the EoS has to be known in the full three-dimensional parameter space to allow for a full description of these physical systems. The computation of the EoS in most of the parameter space is hampered by the infamous sign problem at nonzero density.

In lattice QCD, we are typically working in the grand canonical ensemble, where the densities are traded for the respective chemical potentials. Since in QCD the individual quark densities are conserved, we are free to choose a suitable chemical potential basis. In the $N_f = 2 + 1$ setup, which is sufficient to capture the main dynamics for temperatures around the thermal transition temperature, a convenient basis is given by

$$\mu_u = \mu_L + \mu_I, \quad \mu_d = \mu_L - \mu_I \quad \text{and} \quad \mu_s. \quad (1)$$

This basis is ideally suited to distinguish between cases suffering from the complex action problem and those which do not. As long as $\mu_L = \mu_s = 0$, the case known as pure isospin chemical potential, the action is real and the theory is amenable to Monte-Carlo simulations [4–6]. A few years ago we started the first dedicated program to extract the properties of QCD at non-zero isospin chemical potential at the physical point with controlled systematics. This includes a detailed study of the phase diagram [7, 8], for which the presence of a superconducting BCS phase at large μ_I is still an open question [9, 10], as well as the extraction of the EoS. First accounts of the results for the latter have already been presented for zero [11] and nonzero [3, 12–14] temperatures. Here we will discuss the status of the extraction of the EoS.

A related observable, which has become very prominent in the modelling of the EoS for neutron stars in the past decade, e.g. [15–17], is the speed of sound c_s . In this proceedings article, we will discuss the extraction of the speed of sound from the EoS at zero and non-zero temperature and show the first results for the speed of sound obtained in the pion condensed phase from first principles in full QCD at the physical point. In particular, we will see that for high isospin chemical potentials c_s exceeds the conformal bound [18] of $c_s = 1/\sqrt{3}$. This is the first time that such a behavior has been observed in full QCD within lattice simulations. In light of this, it appears instructive to reconsider what counts as a natural parameter region for c_s .

Eventually, we are interested in the full three-dimensional parameter space. Our simulation points at nonzero isospin chemical potential provide a novel starting point to extract the EoS in this parameter space at small μ_L and μ_s , but large μ_I using indirect methods, giving access to previously inaccessible regions in parameter space. We will discuss the first steps towards the extension of our EoS to $\mu_L \neq 0$ using the Taylor expansion method [19].

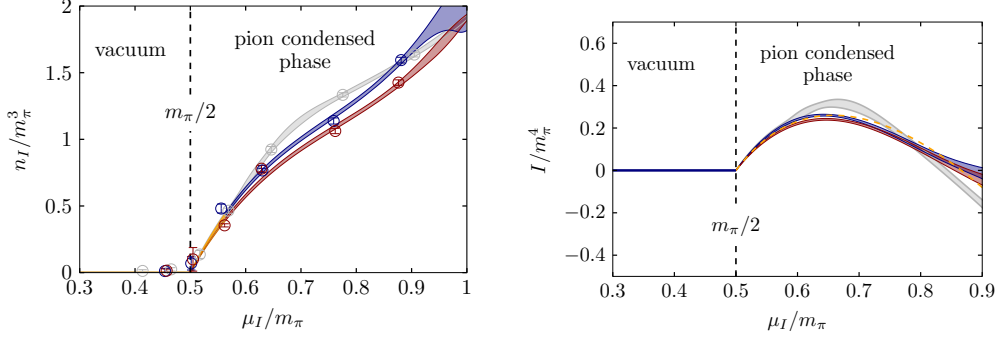


Figure 1: **Left:** Simulation results for the isospin density n_I vs. the isospin chemical potential μ_I at vanishing temperature together with the interpolation explained in the text. The red points and curve belong to the ensembles with $a \approx 0.15$ fm and the blue to the ensembles with $a \approx 0.22$ fm. The light gray results and curves belong to the old data at $a \approx 0.29$ fm and a slightly smaller temperature published in Ref. [11]. **Right:** Results for the interaction measure obtained from the interpolation of the isospin density shown in the left panel. The mapping between colours and lattices is the same as in the left panel. The yellow dashed line is the result from chiral perturbation theory [4].

2. Equation of state at pure isospin chemical potential

In our study, we use $N_f = 2 + 1$ flavours of improved rooted staggered quarks with two levels of stout smearing and tuned to physical quark masses, as well as the tree-level Symanzik improved gluon action. To enable simulations in the phase where charged pions condense, the BEC phase, the simulations entail a regulator, the pionic source, controlled by a parameter λ . In particular, we simulate at $\lambda \neq 0$ and results are extrapolated to $\lambda = 0$ using the improvement program described in Ref. [7]. The relevant observable for the extraction of the EoS is the isospin density

$$\langle n_I \rangle = \frac{T}{V} \frac{\partial \log \mathcal{Z}}{\partial \mu_I}. \quad (2)$$

For the definition and the improvement of the λ -extrapolations we refer to Ref. [11]. In this and the following section we will only discuss results which have already been extrapolated to $\lambda = 0$.

2.1 The EoS at vanishing temperature

The extraction of the EoS at (approximately) vanishing temperature has been discussed in Ref. [11]. The full EoS can be obtained from the isospin density, which, upon integration over μ_I , gives the pressure and the interaction measure,

$$p(0, \mu_I) = \int_0^{\mu_I} d\mu'_I n_I(0, \mu'_I) \quad \text{and} \quad I(0, \mu_I) = -4p + n_I(0, \mu_I) \mu_I. \quad (3)$$

The main problem when extracting the EoS are residual temperature artifacts, due to the missing $T \rightarrow 0$ extrapolations. In practice, we simulate at $T \approx 30$ MeV and correct for the residual effects. Those are mostly prominent in the vicinity of the transition to the BEC phase, see Fig. 1, where they lead to non-vanishing values of the isospin density outside of the BEC phase. We correct these artifacts by applying chiral perturbation theory at non-zero isospin chemical potential [4]

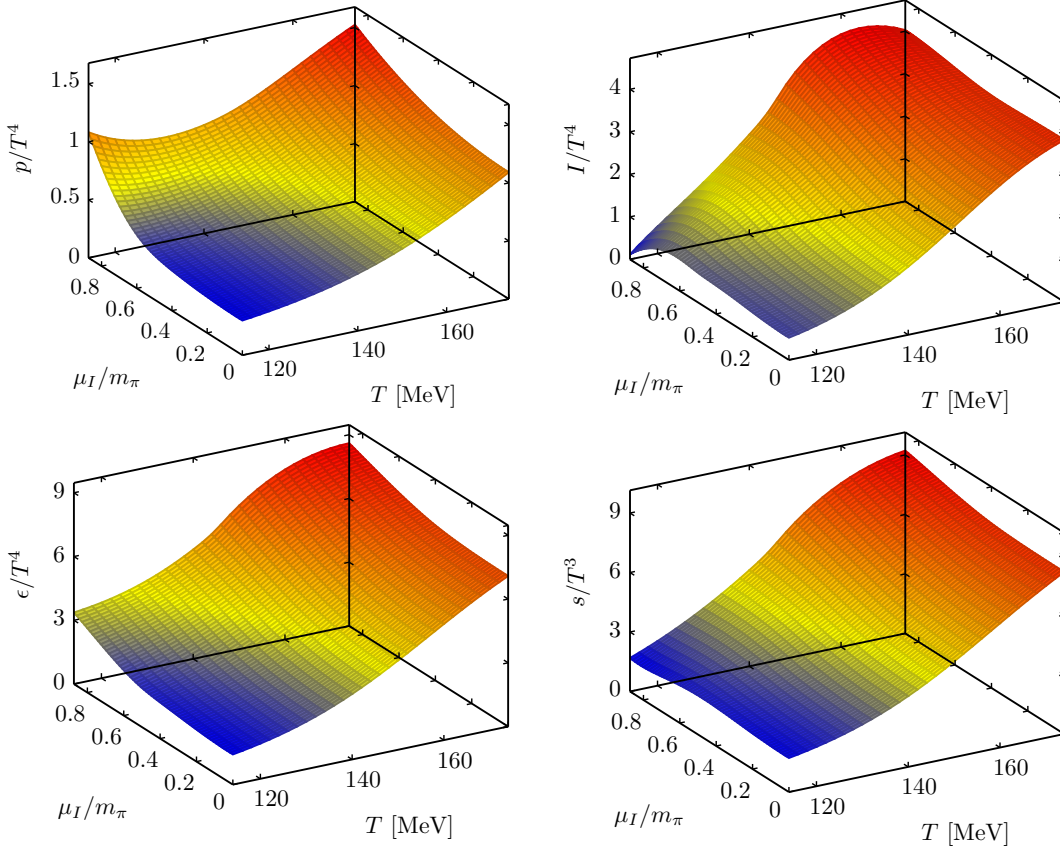


Figure 2: Results for the pressure (top-left), the interaction measure (top-right), the energy density (bottom-left) and the entropy density (bottom-right). The results have been obtained on our lattice with $N_t = 8$ and for better visibility we do not show the uncertainties.

in the vicinity of the transition (see [11]), fitting the first two datapoints in the BEC phase and matching to cubic spline interpolations of the remaining datapoints. The spline interpolations are obtained as model-independently as possible by averaging over spline fits with all possible nodepoint combinations, making use of Monte-Carlo methods [20].

Our study of the EoS at $T = 0$ has been started on a comparably coarse lattice, with $a \approx 0.29$ fm [11]. Here we augment that study with two new sets of ensembles: a set of $24^3 \times 32$ ensembles at a lattice spacing of about $a \approx 0.22$ fm and a set of $32^3 \times 48$ ensembles at $a \approx 0.15$ fm. The results for the interpolation of the isospin density are shown in the left panel of Fig. 1 and the resulting interaction measure in the right panel. The interaction measure shows a clear sign for the presence of the BEC phase. It initially rises until it reaches a maximum around $\mu_I/m_\pi \approx 0.63$ to 0.65 ., from where it decreases until it becomes negative around $\mu_I/m_\pi \approx 0.9$, in good agreement [21] with chiral perturbation theory [4] (yellow dashed line).

2.2 The EoS at nonzero temperature

At $T \neq 0$, we can restrict ourselves to compute the modifications of the pressure and the interaction measure due to the non-vanishing isospin chemical potential, decomposing the two

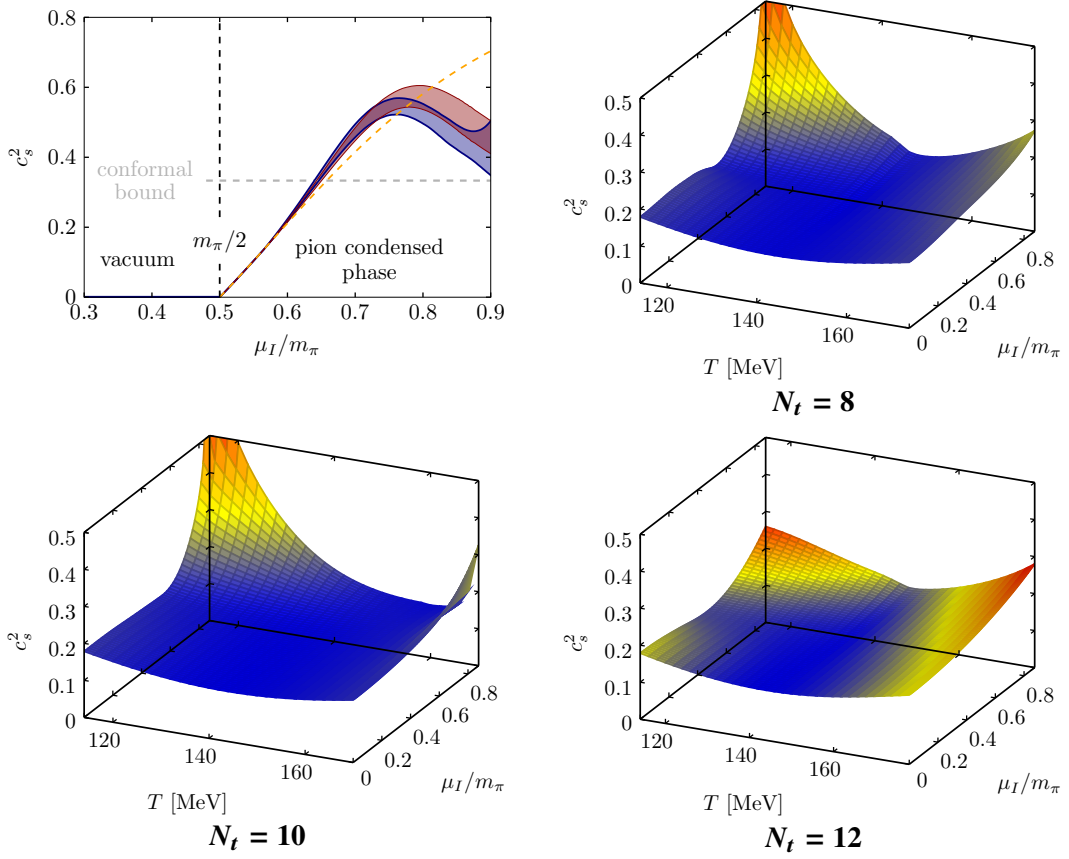


Figure 3: Results for the squared speed of sound at $T = 0$ (top left), with the same color coding as in Fig. 1, and at $T \neq 0$ for $N_t = 8$ (top right), 10 (bottom left) and 12 (bottom right). For the nonzero temperature panels, the uncertainties are again excluded for clearer plots.

quantities as

$$p(T, \mu_I) = p(T, 0) + \Delta p(T, \mu_I) \quad \text{and} \quad I(T, \mu_I) = I(T, 0) + \Delta I(T, \mu_I). \quad (4)$$

The $\mu_I = 0$ contributions are available from the literature [22, 23]. The modifications $\Delta p(T, \mu_I)$ and $\Delta I(T, \mu_I)$ can be computed, similar to the $T = 0$ case, from a, now two-dimensional, interpolation of the isospin density, again using a model independent spline interpolation (see Refs. [3, 14]). After computing the pressure and the interaction measure from the interpolation, most of the other relevant thermodynamic quantities can be computed, such as energy and entropy density, ϵ and s , for instance,

$$\epsilon = I + 3p \quad \text{and} \quad s = \frac{\epsilon + p - \mu_I n_I}{T}. \quad (5)$$

In our study we use the lattices of Ref. [7], to which we refer for further details, which have already been used to map out the phase diagram up to $\mu_I/m_\pi \lesssim 0.9$. In particular, we use the ensembles with $N_t = 8, 10$ and 12 and an aspect ratio $N_s/N_t \approx 3$. From the isospin density we compute modifications of pressure and interaction measure and combine this with the $\mu_I = 0$ data obtained from the interpolation formula provided in Ref. [22] with slightly modified coefficients,

obtained from a reanalysis of the data.¹ The results for the EoS at $T \neq 0$, in particular, the pressure (top left), the interaction measure (top right), the energy density (bottom left) and the entropy density (bottom right), on the $N_t = 8$ ensemble are shown in Fig. 2. Once more we can see the evidence for the presence of the pion condensate in the EoS via the characteristic behavior of the interaction measure at low temperatures. This behavior disappears for temperatures, where the system remains outside the BEC phase even for large μ_I . Similar results for the EoS are also available for $N_t = 10$ and 12, as shown in Ref. [14].

3. The speed of sound

From the above interpolations of the isospin density, one can also extract the isentropic speed of sound c_s , which at non-zero isospin chemical potential is defined as

$$c_s^2 = \left. \frac{\partial p}{\partial \epsilon} \right|_{\frac{s}{n_I} = \text{const}} = \frac{\partial_\xi p}{\partial_\xi \epsilon}. \quad (6)$$

The latter defines the directional derivative in the direction of isentropes, satisfying the condition

$$\partial_\xi \left(\frac{s}{n_I} \right) = 0. \quad (7)$$

For $T = 0$ $\delta_\xi = \delta_{\mu_I}$, while for $T \neq 0$ the directional derivative mixes temperature- and chemical potential-derivatives. Given the spline interpolations, all quantities can be computed analytically.

The results for c_s^2 at $T = 0$ and $T \neq 0$ are shown in Fig. 3. At $T = 0$ (top left panel), the speed of sound increases strongly with μ_I , crosses the conformal bound [18] at $\mu_I/m_\pi \approx 0.64$ and reaches a peak around 0.76 to 0.80. The value of c_s^2 at the peak position is about 0.53 to 0.6. We note, that peak position and the height become larger with decreasing lattice spacing, so that we expect these results to present lower bounds to the continuum limit. Our findings are in good agreement with recent results obtained in two-color QCD [24, 25]. For $T \neq 0$, the remnant of this peak is still visible for $N_t = 8$ and 10, albeit shifted towards larger μ_I values. The tendency for c_s^2 to increase is also still present for $N_t = 12$, but we do not see the crossing of the conformal bound up to $\mu_I/m_\pi = 0.9$. This might be a sign that the peak at $T \neq 0$ gets shifted to even larger μ_I when approaching the continuum limit. Note, however, that the peak appears at the outer sides of the spline interpolations, where results are potentially more affected by systematic uncertainties. For larger temperatures, c_s increases and might even cross the conformal bound at large μ_I values, but to see what is happening in this region further simulations are necessary.

4. Towards an extension to nonzero μ_L via Taylor expansion

We would now like to extend our determination of the EoS to non-zero but small light quark chemical potentials μ_L from Eq. (1). The extension can proceed via a Taylor expansion [19] of the pressure, given by

$$p(T, \mu_I, \mu_L) = \sum_{m=0}^{\infty} \frac{\chi_m^L(T, \mu_I)}{m!} \mu_L^m \quad \text{with} \quad \chi_m^L(T, \mu_I) = \left. \frac{\partial^m p(T, \mu_I, \mu_L)}{\partial \mu_L^m} \right|_{\mu_L=0}. \quad (8)$$

¹We thank Kálmán Szabó for providing the coefficients and their correlations.

The remaining task is to compute the Taylor coefficients for a given point in parameter space (T, μ_I) . Here we will focus on the leading order of the expansion, $m = 2$. The results obtained for different λ of the Taylor coefficient χ_2^L on the $T = 0$ lattices with $a \approx 0.15$ fm are shown in Fig. 4. These results for the Taylor coefficients are unimproved with respect to the λ -extrapolations and, at first glance, seem to facilitate a simple extrapolation to $\lambda = 0$.

In Ref. [7] we have detailed the improved $\lambda \rightarrow 0$ extrapolation procedure for condensates and densities. In the valence quark improvement we generically split the operators associated with light quark fermionic observables by $\langle O \rangle = \langle O - \delta_O^N \rangle + \langle \delta_O^N \rangle$, with $\lim_{\lambda \rightarrow 0} \langle \delta_O^N \rangle = 0$. The improvement term δ_O^N is defined via an approximation of the trace appearing in $O \sim \text{Tr}(\hat{O} M^{-1})$ in terms of singular values and the corresponding eigenstates of the massive Dirac operator, $M^\dagger(\mu_I) M(\mu_I) \varphi_n = \xi_n^2 \varphi_n$, so that

$$\delta_O^N \sim \sum_{n=0}^{N-1} O_{nm} \left(\frac{1}{\xi_n^2 + \lambda^2} - \frac{1}{\xi_n^2} \right), \quad (9)$$

where we have introduced the matrix elements of the operator O with respect to the eigenstates, $O_{nm} = \varphi_n^\dagger \hat{O} \varphi_m$. Here this procedure has to be extended to susceptibilities. Those include traces with two inverses of the Dirac operator, for which the contribution of low modes reads

$$\langle \text{Tr}(\hat{O}_1 M^{-1} \hat{O}_2 M^{-1}) \rangle \approx \left\langle \sum_{n,m=0}^{N-1} \frac{O_{1;nm}}{\xi_m^2 + \lambda^2} \frac{O_{2;mn}}{\xi_n^2 + \lambda^2} \right\rangle, \quad (10)$$

where the matrix elements are defined as above. Using this representation, we can define the improvement term δ_χ^N for the valence quark improvement of a generic susceptibility χ analogous to Eq. (9) as

$$\delta_\chi^N \sim \sum_{n,m=0}^{N-1} O_{1;nm} O_{2;mn} \left(\frac{1}{(\xi_n^2 + \lambda^2)(\xi_m^2 + \lambda^2)} - \frac{1}{\xi_n^2 \xi_m^2} \right). \quad (11)$$

In principle, one could truncate the two sums at different numbers of singular values. This, however, is not beneficial numerically, since the lowest singular value matrix elements are available immediately for all operators. We note that the leading order reweighting of gauge configurations, as developed for condensates in Ref. [7], can be included in the same way.

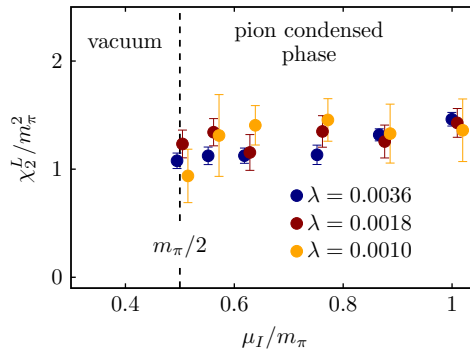


Figure 4: Results for the leading order Taylor coefficient χ_2^L in the BEC phase for different values of λ (indicated in lattice units) obtained on our $T \approx 0$ lattices at $a \approx 0.15$ fm.

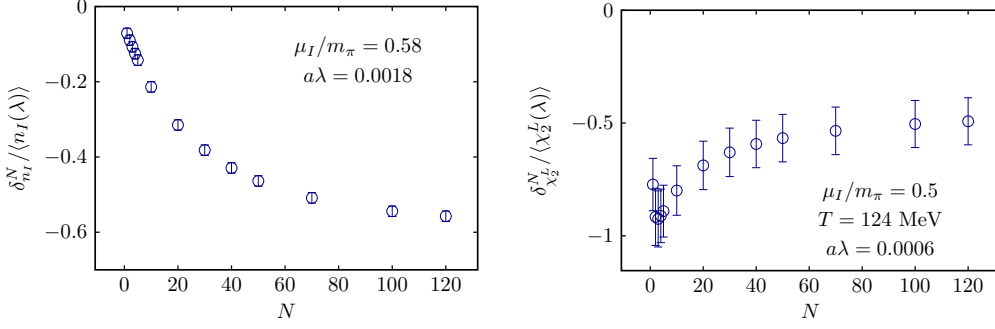


Figure 5: Left: Results for the improvement term of the isospin density versus the number of singular values included in its computation on the $T = 0$ lattice at $a \approx 0.15$ fm with $\mu_I/m_\pi = 0.58$. **Right:** Results for the improvement term of the leading order Taylor coefficient χ_2^L versus the number of singular values included in its computation on one of the $24^3 \times 6$ lattices with $T = 124$ MeV.

We show the results for the improvement term $\delta_{n_I}^N$ for different values of N in the left panel of Fig. 5. When we apply the same procedure for χ_2^L , however, the lowest singular values are found to dominate the improvement term more strongly, since they appear with a higher power in the denominator of Eq. (11). This has two effects: first, it leads to a larger correction term, which, however, becomes visible in the unimproved susceptibilities only at smaller values of λ . Hence the small dependence on λ in Fig. 4. Second, it increases fluctuations in the correction terms and leads to larger uncertainties. This is visible in the right panel of Fig. 5, where we show the improvement term $\delta_{\chi_2^L}^N$ versus N for a nonzero temperature ensemble. We note, that the situation becomes worse at $T \approx 0$, where the dominance of the lowest singular value is observed to be even stronger. This behavior renders reliable λ -extrapolations of the Taylor expansion coefficients more challenging and requires further optimization.

5. Conclusions

In this proceedings article we have presented the status of our study of the EoS of isospin-asymmetric QCD at zero and non-zero temperatures. The EoS has been determined from a model independent spline interpolation of the isospin density and at $T = 0$ residual temperature effects have been corrected using chiral perturbation theory [4] in the vicinity of the transition to the BEC phase. In the BEC phase at small temperatures the interaction measure shows a very distinctive feature: it initially increases until it reaches a maximum, followed by a reduction and eventually turns negative deep in the BEC phase. Another, particularly interesting observable related to the EoS is the isentropic speed of sound. At zero temperature, the speed of sound increases in the BEC phase, exceeds the conformal bound [18] at $\mu_I/m_\pi \approx 0.64$ and exhibits a peak around $\mu_I/m_\pi \approx 0.76$ to 0.80 . The onset of this peak is still visible for small non-zero temperatures on coarser lattices, but it becomes shifted towards larger μ_I values with increasing temperature and in the approach to the continuum limit. To our knowledge this is the first time that a speed of sound larger than the conformal bound has been observed in first principles QCD. Finally, we discussed our preliminary results concerning the impact of small light quark baryon chemical potentials μ_L (cf. Eq. (1)) using Taylor expansion

sion around the novel expansion points at non-zero temperature and isospin chemical potentials. The determination of the corresponding susceptibilities in the zero pion source limit is observed to be more demanding than for simple quark bilinears like the pion condensate or the isospin density.

Acknowledgements:

This work has been supported by the Deutsche Forschungsgemeinschaft (DFG, German Research Foundation) via CRC TRR 211 – project number 315477589. The authors gratefully acknowledge the Gauss Centre for Supercomputing e.V. (www.gauss-centre.eu) for funding this project by providing computing time on the GCS Supercomputer SuperMUC-NG at Leibniz Supercomputing Centre (www.lrz.de).

References

- [1] M. M. Wygas, I. M. Oldengott, D. Bödeker and D. J. Schwarz, *Cosmic QCD Epoch at Nonvanishing Lepton Asymmetry*, *Phys. Rev. Lett.* **121** (2018) 201302 [[1807.10815](#)].
- [2] M. M. Middeldorf-Wygas, I. M. Oldengott, D. Bödeker and D. J. Schwarz, *The cosmic QCD transition for large lepton flavour asymmetries*, [2009.00036](#).
- [3] V. Vovchenko, B. B. Brandt, F. Cuteri, G. Endrődi, F. Hajkarim and J. Schaffner-Bielich, *Pion Condensation in the Early Universe at Nonvanishing Lepton Flavor Asymmetry and Its Gravitational Wave Signatures*, *Phys. Rev. Lett.* **126** (2021) 012701 [[2009.02309](#)].
- [4] D. T. Son and M. A. Stephanov, *QCD at finite isospin density*, *Phys. Rev. Lett.* **86** (2001) 592 [[hep-ph/0005225](#)].
- [5] J. B. Kogut and D. K. Sinclair, *Quenched lattice QCD at finite isospin density and related theories*, *Phys. Rev. D* **66** (2002) 014508 [[hep-lat/0201017](#)].
- [6] J. B. Kogut and D. K. Sinclair, *Lattice QCD at finite isospin density at zero and finite temperature*, *Phys. Rev. D* **66** (2002) 034505 [[hep-lat/0202028](#)].
- [7] B. B. Brandt, G. Endrődi and S. Schmalzbauer, *QCD phase diagram for nonzero isospin-asymmetry*, *Phys. Rev. D* **97** (2018) 054514 [[1712.08190](#)].
- [8] B. B. Brandt and G. Endrődi, *Reliability of Taylor expansions in QCD*, *Phys. Rev. D* **99** (2019) 014518 [[1810.11045](#)].
- [9] B. B. Brandt, F. Cuteri, G. Endrődi and S. Schmalzbauer, *The Dirac spectrum and the BEC-BCS crossover in QCD at nonzero isospin asymmetry*, *Particles* **3** (2020) 80 [[1912.07451](#)].
- [10] F. Cuteri, B. B. Brandt and G. Endrődi, *Searching for the BCS phase at nonzero isospin asymmetry*, *PoS LATTICE2021* (2022) 232 [[2112.11113](#)].
- [11] B. B. Brandt, G. Endrődi, E. S. Fraga, M. Hippert, J. Schaffner-Bielich and S. Schmalzbauer, *New class of compact stars: Pion stars*, *Phys. Rev. D* **98** (2018) 094510 [[1802.06685](#)].

- [12] B. B. Brandt, G. Endrődi and S. Schmalzbauer, *QCD at finite isospin chemical potential*, *EPJ Web Conf.* **175** (2018) 07020 [[1709.10487](#)].
- [13] B. B. Brandt, G. Endrődi and S. Schmalzbauer, *QCD at nonzero isospin asymmetry*, *PoS Confinement2018* (2018) 260 [[1811.06004](#)].
- [14] B. B. Brandt, F. Cuteri and G. Endrődi, *QCD thermodynamics at non-zero isospin asymmetry*, *PoS LATTICE2021* (2022) 132 [[2110.14750](#)].
- [15] I. Tews, J. Carlson, S. Gandolfi and S. Reddy, *Constraining the speed of sound inside neutron stars with chiral effective field theory interactions and observations*, *Astrophys. J.* **860** (2018) 149 [[1801.01923](#)].
- [16] E. Annala, T. Gorda, A. Kurkela, J. Nättilä and A. Vuorinen, *Evidence for quark-matter cores in massive neutron stars*, *Nature Phys.* **16** (2020) 907 [[1903.09121](#)].
- [17] M. Marczenko, L. McLerran, K. Redlich and C. Sasaki, *Reaching percolation and conformal limits in neutron stars*, [2207.13059](#).
- [18] A. Cherman, T. D. Cohen and A. Nellore, *A Bound on the speed of sound from holography*, *Phys. Rev. D* **80** (2009) 066003 [[0905.0903](#)].
- [19] S. A. Gottlieb, W. Liu, D. Toussaint, R. L. Renken and R. L. Sugar, *Fermion Number Susceptibility in Lattice Gauge Theory*, *Phys. Rev. D* **38** (1988) 2888.
- [20] B. B. Brandt and G. Endrődi, *QCD phase diagram with isospin chemical potential*, *PoS LATTICE2016* (2016) 039 [[1611.06758](#)].
- [21] P. Adhikari and J. O. Andersen, *QCD at finite isospin density: chiral perturbation theory confronts lattice data*, *Phys. Lett. B* **804** (2020) 135352 [[1909.01131](#)].
- [22] S. Borsányi, Z. Fodor, C. Hoelbling, S. D. Katz, S. Krieg and K. K. Szabó, *Full result for the QCD equation of state with 2+1 flavors*, *Phys. Lett. B* **730** (2014) 99 [[1309.5258](#)].
- [23] HotQCD collaboration, *Equation of state in (2+1)-flavor QCD*, *Phys. Rev. D* **90** (2014) 094503 [[1407.6387](#)].
- [24] K. Iida and E. Itou, *Velocity of Sound beyond the High-Density Relativistic Limit from Lattice Simulation of Dense Two-Color QCD*, [2207.01253](#).
- [25] E. Itou and K. Iida, *Bump of sound velocity in dense 2-color QCD*, in *39th International Symposium on Lattice Field Theory*, 10, 2022, [2210.14385](#).